Sessini, V. et al., 2016. Processing of edible films based on nanoreinforced gelatinized starch. Polymer Degradation and Stability, 132, pp.157–168.

PROCESSING OF EDIBLE FILMS BASED ON NANOREINFORCED GELATINIZED STARCH

Valentina Sessini[1], Marina P. Arrieta[2], José Maria Kenny[1,2] and Laura Peponi[2*]

[1] Dipartimento di Ingegneria Civile e Ambientale, Università di Perugia, Strada di Pentima, 05100 Terni, Italy, valentina.sessini@studenti.unipg.it, jose.kenny@unipg.it

[2] Instituto de Ciencia y Tecnología de Polímeros, ICTP-CSIC., calle Juan de la Cierva 3, 28006, Madrid, Spain, lpeponi@ictp.csic.es, marrieta@ictp.csic.es

*corresponding author: Laura Peponi, lpeponi@ictp.csic.es

ABSTRACT

Fully biobased edible films were prepared using native potato starch plasticized with glycerol and further reinforced with catechin (Cat) and starch nanocrystals (SNC) obtained by acidic hydrolysis from waxy maize starch granules. The thermal stability of starch nanocrystals obtained at different pH was studied, resulting on a decreasing in thermal stability at higher pH values. The X-ray diffraction patterns of the plasticized reinforced materials display complete destructuration of starch by solvent casting process. Plasticized films showed lower onset degradation temperatures than non-plasticized starch film. The reduction of the inter- and intra-molecular bonds interaction within the polymer matrix due to glycerol presence leads to a decrease of the thermal stability of the whole system. On the other hand, Cat and SNC produced an increase of the thermal stability of the bionanocomposites delaying the beginning of the thermal decomposition of starch/glycerol systems of about 20 ºC. The mechanical performance

was also improved in the ternary bionanocomposite edible films. All the edible films were fully disintegrated in compost conditions suggesting their possible applications as biodegradable edible films for packaging.

Keywords: starch, starch nanocrystals, catechin, edible films, biodegradability

1. Introduction

The potential of biodegradable polymers, and in particular of polymers obtained from agro-resources, has been widely investigated during the last few years as alternatives to non-degradable polymers currently used in films production for food packaging [1]. Moreover, the increasing interest toward the reduction of the environmental impact produced by plastic waste, in particular from the food packaging sector, has lead both research and industry to increase their attention on the development of new biodegradable materials [2]. In this sense, one of the most promising raw materials for biodegradable food packaging production is starch, in particular in its thermoplastic form [3]. In fact, among the biomaterials present today in the market, those derived from renewable resources such as starch-based products are the most widespread and economic biomaterials. Starch is currently produced in a large industrial scale and presents an interesting balance of properties [4]. It is mainly composed by two structurally distinct α-D-glucan components: amylose, which is linear, and amylopectin, which is highly branched [5]. Although starches from different botanical origins have identical structural units, their different amylose and amylopectin contents mainly influence its physical and chemical properties. Moreover, it is well known that, depending on the botanic origin of starch (i.e. potato, maize, pea, rice,

wheat, cassava, waxy maize, amylomaize, etc.), native granules present a wide variety of size (2–100 μm), size distribution, shape, extraction from plant conversion factors and chemical composition [1, 6]. Moreover, amylose content as well as its botanic origin considerably influences its crystalline organization [6]. Indeed, several crystalline structures are formed depending on the source of the starch: A (cereal starch), B (tuber starch), C (a combination of A and B crystals), V (retrograded starch) type [7]. Although amylose and the branching regions of amylopectin form the amorphous domains in the starch granule, amylopectin, arranged in double helix organization, is the dominating crystalline component in native starch [1].

Starch can be used alone as a matrix or by blending with other bio-polymers in several bio-applications such as food, food packaging and agriculture [8, 9]. Furthermore, starch, like cellulose, is another renewable natural polysaccharide that can be used to produce nanocrystals (SNC) by means of acid hydrolysis [6, 10, 11]. Moreover, in order to extend starch applications as polymer matrix, it requires water dispersion and its partial or complete gelatinization, thus considering that water acts as destructuring agent. Meanwhile, the combination of high water content and heat leads to the starch granule swelling and therefore the starch gelatinization through the disruption of the granule organization [1]. Although starch is not truly a thermoplastic polymer, it can be transformed into a continuous polymeric entangled phase by mixing with high water content or plasticizer [12]. However, the hydrophilic nature of thermoplastic starches makes them susceptible to moisture attack and resultant changes in dimensional stability and mechanical properties can occur. In addition, depending on the storage conditions of thermoplastic starches, retrogradation of the mobile starch chains lead to an undesired change in the thermo-mechanical performances of the final starch-based material [12, 13]. Moreover, thermoplastic starches are highly brittle limiting their

processing and industrial applications. However, the brittleness of starches are frequently overcome by the addition of plasticizers to get the flexibility required for film applications [14, 15]. Glycerol is a natural plasticizer widely added to develop edible films with the main objective to reduce the film brittleness by reducing intra and intermolecular hydrogen bonds [3, 16, 17]. Moreover, glycerol is the major by-product in biodiesel production and, thus, the use of glycerol as plasticizer for edible films, offers the opportunity to increase its value from a low-grade by-product to a useful plasticizer [18].

On the other hand, a new approach is growing up in the edible films for food packaging applications focused on the development of biobased composites. The addition of fillers, both micro and nano, can considerably improve the thermo-mechanical performance of biobased polymers [19]. Catechin, one of the major active constituents of green tea, is a natural food grade antioxidant, frequently used in the food packaging sector, with the double function to protect polymer matrices during thermal processing and for the development of active packaging materials [2, 20, 21]. In fact, catechin has proven to improve the thermo-mechanical performance of both, traditional plastics such as polypropylene [21] and biopolymers such as poly(lactic acid) (PLA) and poly(hydroxybutyrate) (PHB) [2].

However nanocomposites and in particular bionanocomposites are an interesting class of composites that show improved properties due to the addition of the nanofillers which present a large surface area for a given volume that consequent develop a huge interfacial area between them and the polymer matrix [22, 23]. Bionanocomposites are also reinforced with bionanofillers obtained from renewable resources, e.g., cellulose, starch, and proteins [24]. Due to the fact that starch is abundant in nature at low cost, the use of SNC has recently gained interest as a renewable and biodegradable nanofiller

[24]. Particularly, those SNC obtained by the hydrolysis of native granules of waxy maize starches, since this source is rich in amylopectin (> 99 %). Moreover, in term of food packaging, platelet with square-like shape should be preferred for barrier properties [10].

The main objective of the present work was to develop biodegradable edible films based on gelatinized starch with catechin as antioxidant agent and starch nanocrystals as nanofillers. These systems were plasticized with glycerol with the objective of overcome the ductility required for flexible film applications. The developed materials were characterized with regard to their structure, mechanical and thermal properties with the aim to evaluate their suitability as possible materials for the food packaging sector. Additionally, the disintegrability under composting of the edible films was evaluated to get information about their post-use.

2. Experimental

2.1. Materials

Native potato starch was kindly supplied by Novamont. Glycerol and catechin dehydrate were purchased from Panreac Quimica (PRS) and Sigma-Aldrich, respectively. Waxy maize starch (N200) used to synthesize the SNC, was supplied by Roquette Laisa (Spain). Sulfuric acid (H_2SO_4) was purchased from Sigma-Aldrich.

2.2. Starch nanocrystals (SNC) synthesis

Starch nanocrystals were synthesized by acid hydrolysis. Waxy maize starch granules were mixed with 175 mL of 3.16 M sulfuric acid solution. The suspension was kept under 100 rpm mechanical stirring at 40 ºC, using a silicon oil bath, for 5 days. The final suspensions were washed by successive centrifugations in distilled water (10,000 rpm for 10 minutes) until reaching neutral pH and redispersed using Ultra Turrax for 5

min to avoid aggregates. The obtained suspensions were filtered on a filter tissue (113 Whatman) and storage at 4 ºC [25]. Finally, it was freeze-dried (LIOALFA 6, Telstar) to obtain SNC powder.

In order to study how the pH of the SNC suspension can affect the thermal stability of SNC three different pH values were studied, that is, 7, 9 and 11.

2.3. Film preparation

Thermoplastic starch was successfully obtained by gelatinization of an aqueous dispersion of 1 wt % of potato starch powder. Glycerol, used as plasticizer, was added in the starch dispersion at three different concentrations, 15, 25 and 35 wt % relative to the mass of potato starch. Then, the mixture was heated at 80 ºC for 15 minutes under continuous stirring. The edible films were obtained by solvent casting method in a polystyrene petri dish and evaporated in a ventilated oven at 35 ºC for 24 h to obtain films with a thickness between 50 and 100 µm. Unplasticized sample was prepared in the same way for comparison, named S-Gly0. The higher glycerol concentration, 35 wt %, named S-Gly35, was chosen to prepare the edible films. So, biocomposite edible films were obtained by adding catechin (1 wt % relative to the mass of potato starch) as antioxidant agent, S-Gly35-Cat, while bionanocomposites edible films were obtained adding starch nanocrystals (1 wt % relative to the mass of potato starch) as bionanofillers, S-Gly35-SNC . Moreover, the synergetic effect of both catechin and SNC was evaluated in the bionanocomposite edible films obtained by adding both catechin and SNC at 1 wt %, S-Gly35-Cat-SNC. Catechin was added before of the gelatinization process in order to ensure a good dispersion and a better interaction with starch. Whereas SNC were added when the temperature of gelatinized starch fell down to 40 ºC to avoid the gelatinization of the SNC [11]. After that, the mixture was stirred

for 1 hour and it was cast to obtain the edible films. The composition of the different samples studied is reported in Table 1.

Table 1. Edible films composition.

Sample	Starch content (wt %)	Glycerol content (wt %)	Catechin (wt %)	SNC (wt %)
S-Gly0	100	-	-	-
S-Gly15	85	15	-	-
S-Gly25	75	25	-	-
S-Gly35	65	35	-	-
S-Gly35-Cat	65	34	1	-
S-Gly35-SNC	65	34	-	1
S-Gly35-Cat-SNC	65	33	1	1

2.4. Characterization techniques

Thermogravimetric analysis (TGA) was carried out using a TA-TGA Q500 thermal analyzer. SNC were tested using about 7 milligrams of sample from room temperature to 800 ºC at 10 ºC min^{-1} under nitrogen atmosphere with a flow of 60 mL min^{-1}. In particular, TGA of SNC suspensions at pH 7, 9 and 11 was conducted in order to evaluate the influence of pH in their thermal stability.

The edible films were analyzed by both isothermal mode under air atmosphere and by dynamic mode under nitrogen atmosphere. Sample weights were around 5-10 mg. Isothermal tests were carried out at 110 ºC during 50 min while dynamic measurements were run from 30 to 600 ºC at 10 ºC min^{-1}. The initial degradation temperatures (T_{10}%) were determined at 10 % of mass loss, whereas temperatures at the maximum

degradation rate (T_{max}) were calculated from the first derivative of the TGA curves (DTG).

The SNC dispersion and shape were observed by Field Emission Scanning Electron Microscope (FE-SEM, Hitachi S8000) in transmission mode. The cryo-fracture surfaces of all the edible films (unfilled films, biocomposites and bionanocomposite) were studied by Scanning Electron Microscopy (SEM PHILIPS XL30 with a tungsten filament). The edible films were previously frozen using liquid N_2 and then cryo-fractured. All the samples were gold/palladium coated by an automatic sputter coater Polaron SC7640 previous to be observed.

Attenuated total reflectance - Fourier transform infrared spectroscopy (ATR-FTIR) measurements were carried out with a Spectrum One FTIR spectrometer (Perkin Elmer instruments). Spectra were obtained in transmission mode at room temperature in the 4000-650 cm^{-1} region with a resolution of 4 cm^{-1} and 32 scans.

X-ray Diffraction (XRD) measurements were performed using a Bruker D8 Advance instrument with a Cu K_α source (0,154 nm) and a detector Vantec1 in order to study the starch crystalline type structure. The scanning range was 2º- 45º, step-size and count time per step were 0.023851º and 0.5 seconds, respectively.

The starch gelatinization temperature was determined by Differential Scanning Calorimetry (DSC) analysis. The dynamic DSC measurements were performed in a Mettler Toledo DSC822e instrument under nitrogen flow (30 ml min^{-1}). Samples of about 10 mg were sealed in aluminum pans. Thermal cycle was just composed by the first heating at 10 ºC min^{-1} from room temperature to 85 ºC.

The mechanical properties were determined using an Instron Universal Testing Machine at a strain rate of 10 mm min^{-1}. Tensile test measurements were performed on 5 dog-bone specimens with a width of 2 mm and leaving an initial length between the

clamps of 15 mm. From these experiments the Young Modulus, as the slope of the curve between 0 % and 2 % of deformation, the elongation at break and the tensile strength at break were obtained. Edible films were disintegrated in composting conditions at laboratory scale level according to the ISO 20200 standard [26]. Edible films were cut in 15 mm × 15 mm and buried at 4-6 cm depth in perforated plastic boxes containing a solid synthetic wet waste consisting in 10 % of compost (Mantillo, Spain), 30 % rabbit food, 10 % starch, 5 % sugar, 1 % urea, 4 % corn oil and 40 % sawdust and approximately 50 wt % of water content. The boxes were incubated at aerobic conditions at 58 ºC. Then, edible films were recovered at 0.5, 1.5, 6, 8 and 30 h of the disintegration test, dried in an oven at 37 ºC during 24 h and reweighed. Photographs of recovered samples were taken for visual comparison. The disintegration degree was calculated by normalizing the sample weight, at different hours of incubation, to the initial weight.

3. Results and discussion

3.1. SNC Characterization

In order to check if the acid hydrolysis treatment effectively led to remove the amorphous domains of starch granules while leaving the crystalline part intact, the crystalline profile of SNC was evaluated by X-ray diffraction pattern. It has been suggested that depending on their X-ray diffraction pattern, starches are categorized in three crystalline types called A, B and C [7, 27-29]. Imberty at al. [28, 29] proposed a model for the double helices packing configuration to explain differences between A- and B-type starches. A-type structures [13] are closely packed with water molecules between each double helical structure, whereas B-type are more open and water molecules are located in the central cavity formed by six double helices. C-type starch pattern presents a mixture of both A- and B-type [7, 27]. This difference in crystalline

structure could render different nanocrystals morphology. In this work the X-ray pattern for native starch granule, named WMS, and of their respective SNC, named WMSNC, are shown in Fig. 1.a. X-ray pattern of native waxy maize starch as well as of SNC displays all the characteristic peaks of the A-type structure (2θ = 9.9º, 11.2º, a strong intensity peak at 15º, a double peak at 17º and 17.7º and a last strong intensity peak at 22.9º).

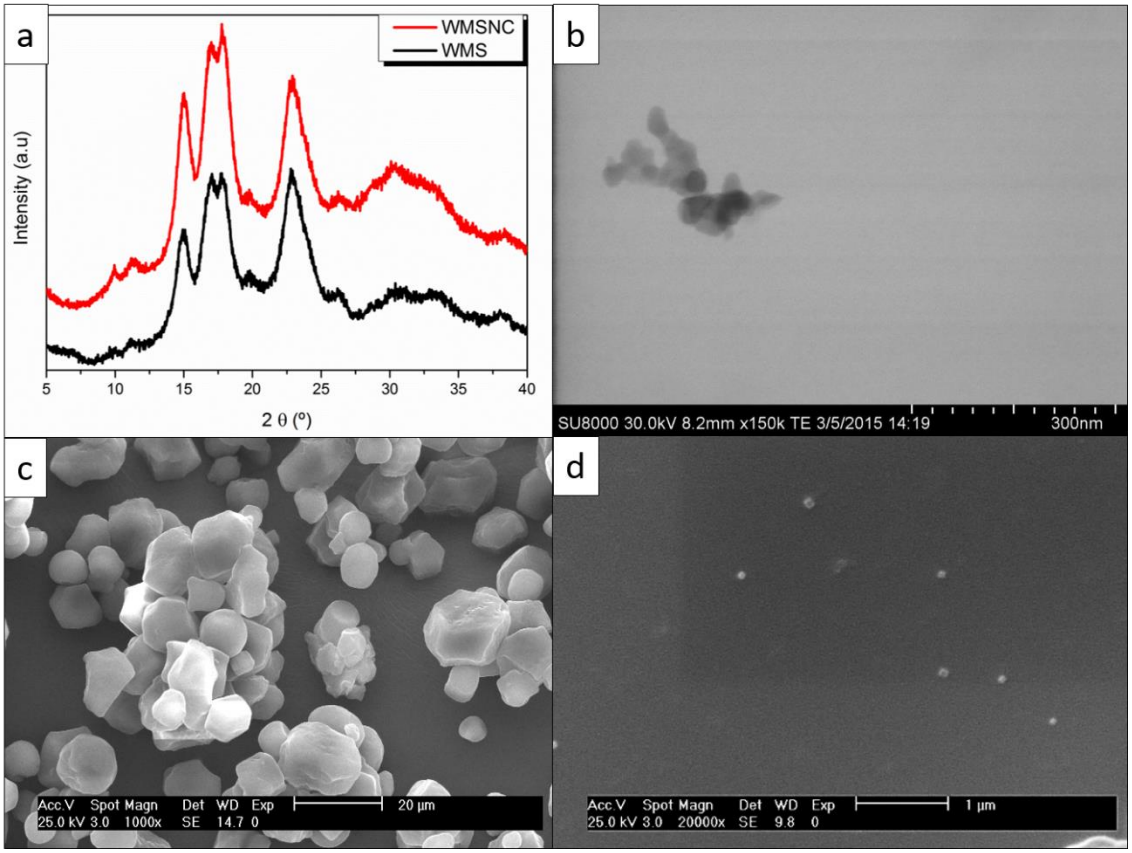

Fig. 1. Comparison of shape and crystalline structure between native waxy maize starch and its SNC. (a) X-ray patterns of WMS and WMSNC, (b) FE-SEM image of WMSNC at pH 7. SEM images of (c) WMS granules and (d) WMSNC at pH 7.

In Fig. 1.b and Fig. 1.d the FE-SEM image and SEM image of waxy maize SNC is reported, respectively, showing square-like particles. Their morphology is in good agreement with their crystalline type. In fact, as previously reported by LeCorre at al.

[6] nanocrystals produced from A-type starches rendered square-like particles, whereas nanocrystals produced from B-type starches rendered round-like particles. Fig. 1.c shows the SEM image obtained for native starch granules where it is worth to note that native starch granules display different shapes, sizes and size distribution.

Thermogravimetric analysis of freeze-dried SNC obtained from suspensions at different pH was carried out in order to study the influence of the pH on the thermal stability of SNC. TGA results are reported in Fig. 2 where the weight loss vs. temperature and the derivative curves (DTG) are shown.

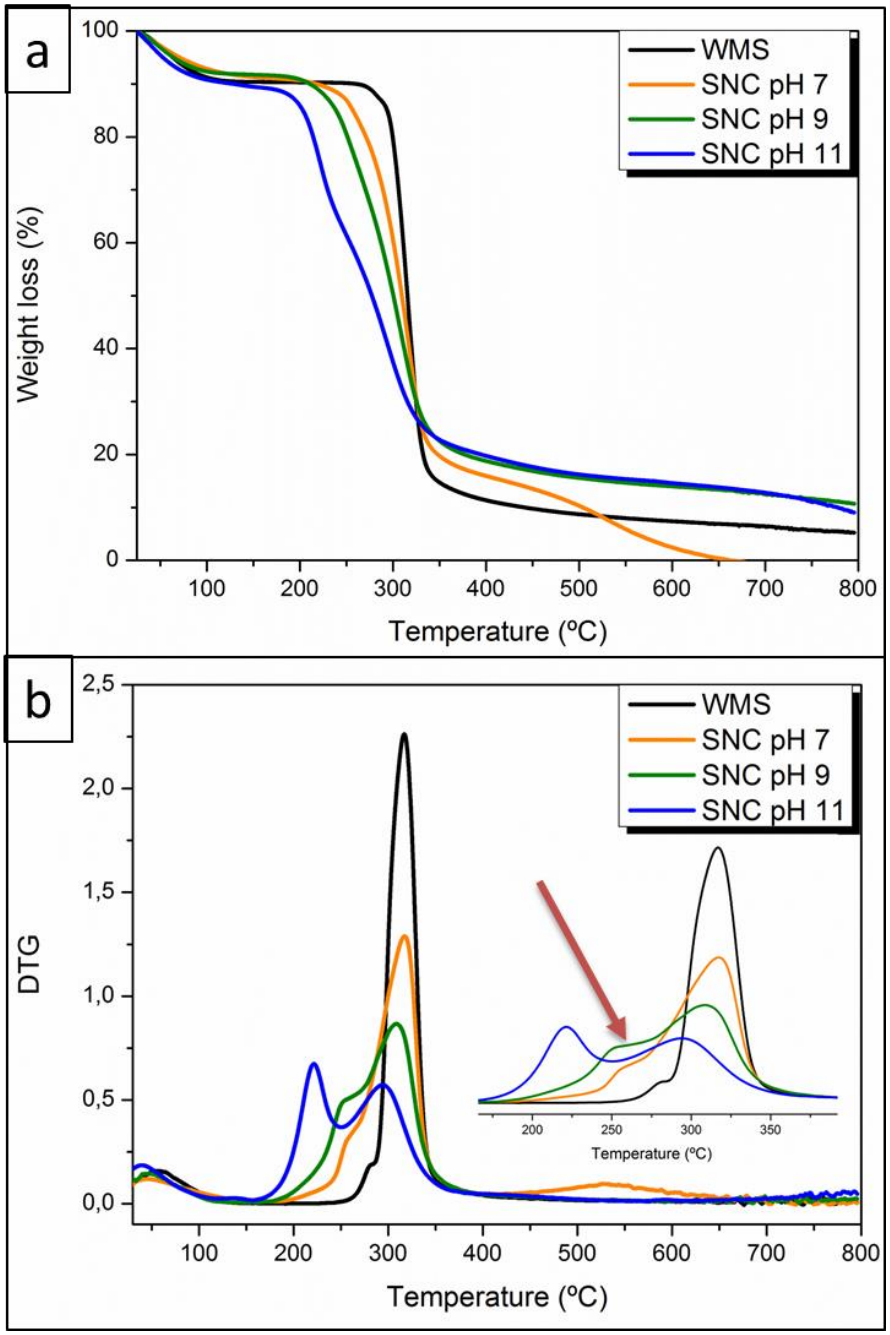

Fig. 2. Thermogravimetric analysis of SNC at different pH values: a) TGA and b) DTG.

SNC at pH 7 showed the initial degradation temperature ($T_{10\%}$) at 218 ºC, while WMS showed it at about 260 ºC. The maximum degradation temperature (T_{max}) was about 317 ºC for both, with a small shoulder at lower temperatures of 280 ºC for WMS and at around 256 ºC for SNC. It can be observed that increasing the pH, the small shoulder increased and it was shifted to lower values. This behaviour can be related with the

SNC surface modification which leads to surface components with higher reactivity [30]. SNC depolymerization starts earlier than native starch [9]. This is attributed to the presence of sulfate groups on the surface of SNC which catalyze the depolymerization reaction [11] Wei et al., varying the pH of SNC from 6.5 to 10.6, reported that the degradation of sulfate esters under alkaline condition contributed to the increase of the zeta-potential of SNC suspension and consequently leading to a more stable suspension and much smaller and narrower particle size distribution [31].

In this work the pH of SNC suspension was also adjusted to 9 and 11 with dilute NaOH in order to compare their thermal stability with those obtained at pH 7. A more stable suspension with a better particle size distribution was obtained at pH 11 as reported in the images in Fig. 3-b and c, in well agreement with Wei et al. [31].

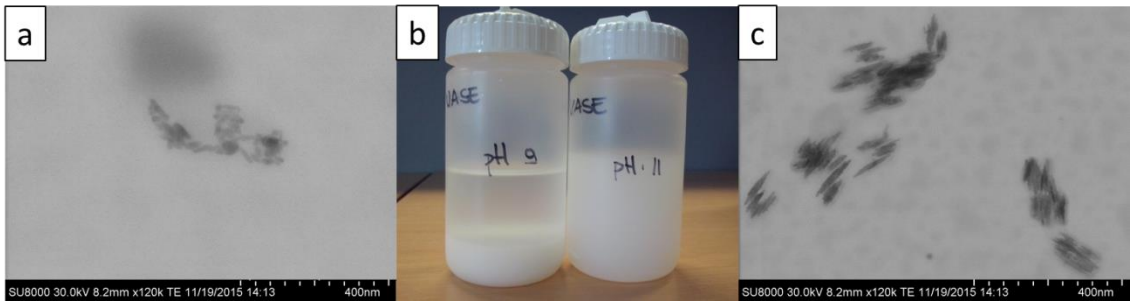

Fig. 3. FE-SEM images of SNC dispersion at (a) pH 9 and (c) pH 11 and sedimentation properties (b).

However, in term of the thermal stability, the increase on pH values showed higher decreases on the onset degradation temperature (SNC at pH 9 $T_{10\%}$ = 211 ºC and SNC at pH 11 $T_{10\%}$ = 129 ºC) and the maximum degradation temperature (SNC at pH 9 T_{max} = 309 ºC and SNC at pH 11 T_{max} = 295ºC). The shoulder of the maximum degradation temperature was also shifted to lower temperatures (252 ºC) in the case of pH 9, while for pH 11 it resulted in a peak centered at 220 ºC.

The TGA results show that the increase on pH dispersion produced a decrease of the onset degradation temperature moving up the beginning of the thermal decomposition. These results could be explained by the smaller size distribution of SNC dispersion at pH 11 and thus the specific surface area is bigger and more sulfate groups can catalyze the depolymerization reaction. However, from TGA thermograms it is worth to note that all SNC obtained at the three different pH values were substantially thermally stable in the region below 125 ºC. Consequently, from these results it is possible to point out that SNC at pH 7 are suitable for to be used in dry processing methods where temperature does not exceed 180 ºC. On the other hand in wet process, where it is not possible to exceed the gelatinization temperature of the SNC, it could be possible to use also the SNC at pH 11. However, in the present work we processed the edible films by means of the solvent casting technique and the selected pH for SNC was 7 since these edible films are intended for the food packaging sector where bionanocomposites should be compounded and processed by melt blending technologies for further industrial applications.

3.2. Processing of the edible films

It is well known that starch materials suffer a gelatinization process, in excess of water, (80 wt %) to obtain a homogeneous material [32, 33]. Thus, with the main objective to obtain a homogeneous material, DSC analysis was carried out for native potato starch with an excess of water (Fig.4.a), in order to select the right temperature for the solvent casting processing.

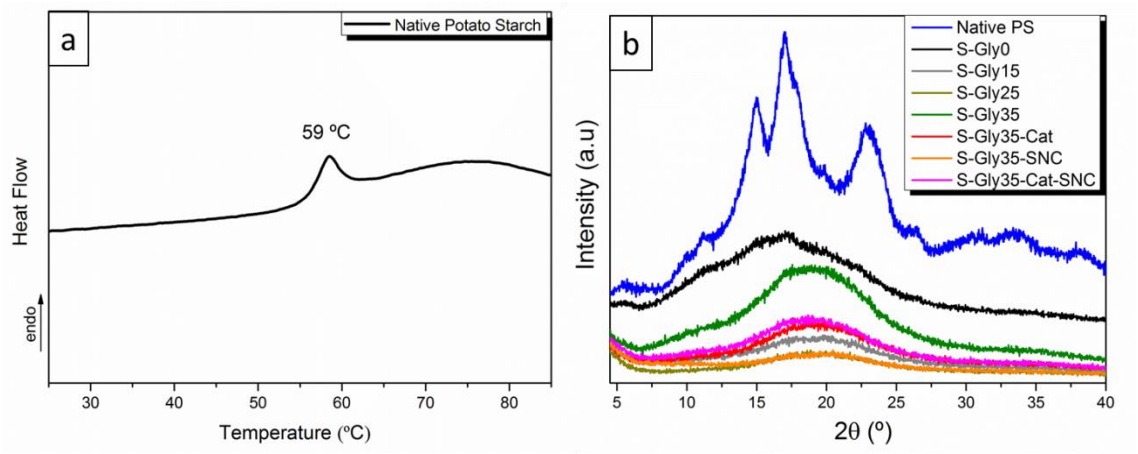

Fig. 4. (a) First scan of DSC analysis for the native potato starch in excess of water, and (b) XRD analysis of native potato starch and all the edible films obtained.

The DSC analysis shows the gelatinization peak of potato starch, which presents its maximum centered at 59 ºC. According with the literature [34, 35] the irreversible swelling of potato starch granules occurs above 60 ºC. Therefore, in this work, in order to obtain the complete starch granules destructuration the temperature selected for solvent casting process was 80 ºC for 15 minutes. The crystalline structure of the developed films as well as of the native potato starch (PS) was investigated by XRD (Fig. 4.b). X-ray pattern of native potato starch displays all the characteristic peaks of the B-type structure (2θ = 5.52º, 11.18º, 15º, 17.04º, 22.93º, 26.35º, 30.90º and 33.39º) [36, 37]. Furthermore Fig. 4.b shows that the crystalline structure of native starch granules has disappeared during the solvent casting process. This result confirms that the complete granules destructuration has been reached at the selected processing conditions. Transparent edible films were successfully obtained by following the above-described procedure. Fig. 5 shows, as example, the obtained plasticized edible film with 35 wt % of glycerol, S-Gly35 (Fig. 5.a), the bionanocomposite edible film reinforced

with SNC, S-Gly35-SNC (Fig. 5.b) and the bionanocomposite with both, SNC and Cat, S-Gly35-Cat-SNC (Fig. 5.c).

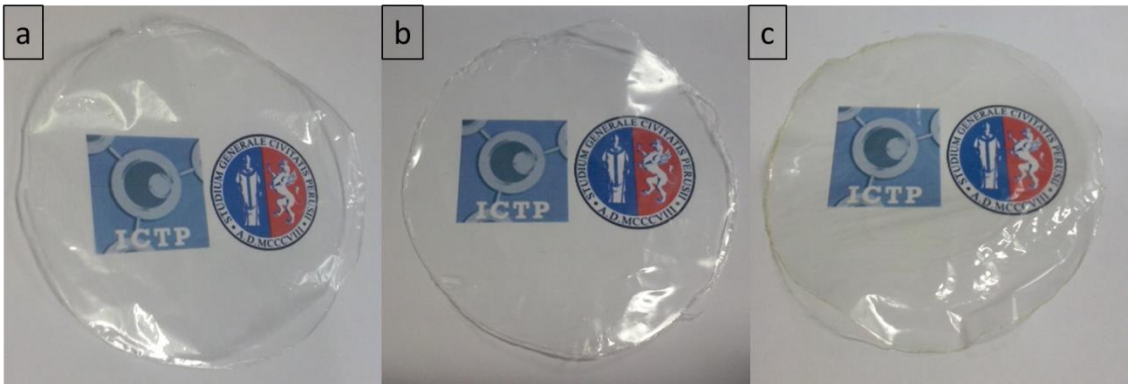

Fig. 5. Visual appearance of the obtained edible films: (a) S-Gly35, (b) S-Gly35-SNC, and (c) S-Gly35-Cat-SNC.

All the edible films are transparent, however, samples containing catechin showed a slightly orange tone.

3.3. Edible Film Characterization

Fig. 6 shows the FTIR measurements for plasticized and unplasticized films in different regions (Fig. 6.a and b) as well as for the biocomposite and bionanocomposites edible films (Fig. 6.c and d). All the starch based films showed the band from 3200 to 3400 cm^{-1} related with the stretching of intermolecular and intramolecular bonds of starch hydroxyl groups (Fig. 6.a and c) [38]. As expected, the intensity of this band increased with glycerol concentration, while it seems to decrease in S-Gly35 based biocomposites and bionanocomposites due to the lower proportion of glycerol in the final formulations due to the incorporation of Cat and SNC (Fig. 6.c). Similarly, the asymmetric and symmetric stretching vibrations of C-H bonds at and 2925 cm^{-1} and the shoulder at 2885 cm^{-1} as well as the bands related to the primary (1080 cm^{-1}), secondary (1100 cm^{-1}) and

tertiary (1150 cm^{-1}) alcohols showed higher intensities when glycerol concentration increased (Fig. 6.b). They also seem to decrease in S-Gly35 based biocomposites and bionanocomposites due to the lower proportion of glycerol in the final formulations (Fig. 6.d). At 1645 cm^{-1} appeared the O-H bending of absorbed water in all starch based films (Fig. 6.b and 6.d) [39]. No significant differences were observed between S-Gly35 film and the biocomposites as well as the bionanocomposites in the FTIR spectra, probably owing to the low amount of SNC and Cat added in the present study.

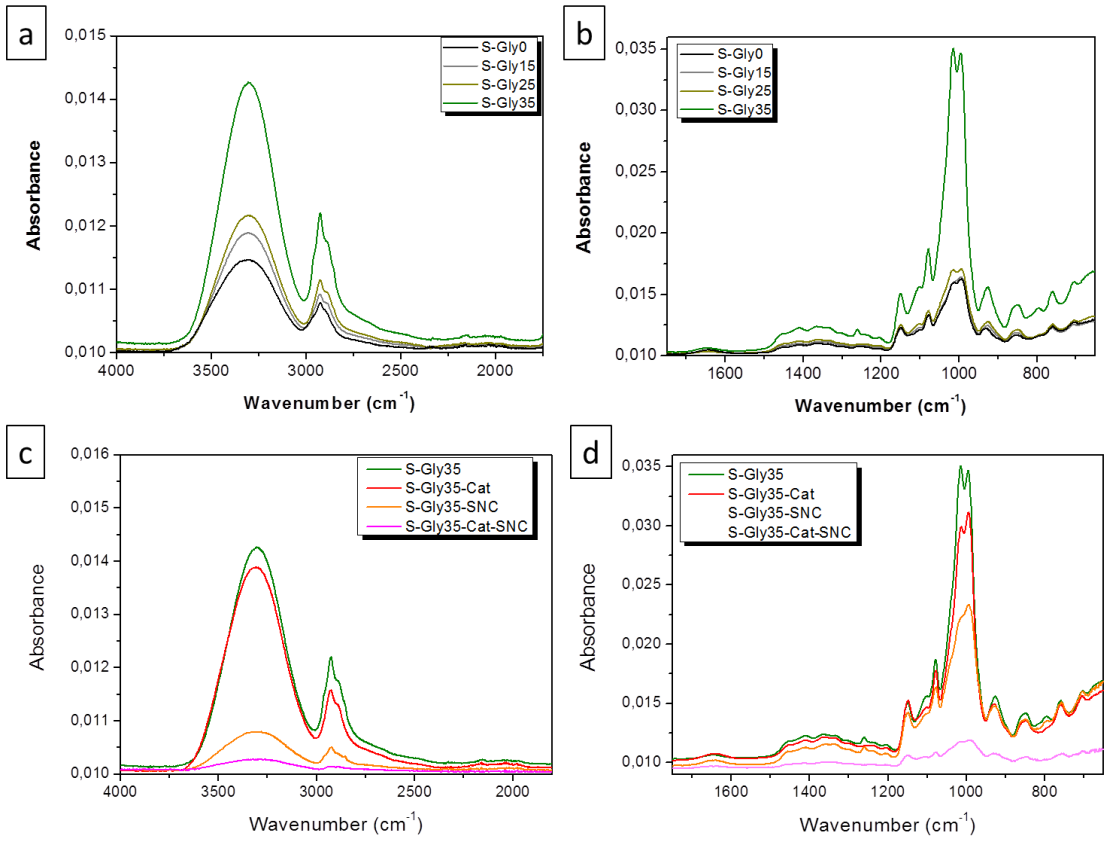

Fig. 6. FTIR spectra of unplasticized starch and plasticized starch films: (a) in the 4000 -1800 cm^{-1} and (b) 2000-650 cm^{-1} region.

S-Gly35, the edible films: (c) in the 4000 -1800 cm^{-1} and (d) 2000-650 cm^{-1} region.

The cryo-fractured surfaces of all the edible films were studied by SEM (Fig. 7.) in order to evaluate the influence of the addition of glycerol, catechin and starch nanocrystals on their microstructure. SEM images of cryo-fractured surfaces of unplasticized and plasticized edible films, with the different amount of glycerol, are reported in Fig.7.a, b, c and d, respectively. All the edible films showed a smooth fracture. No significant differences were observed between the edible films with different amount of glycerol and the unplasticized counterpart. No apparent phase separation is observed, confirming the homogeneous dispersion of glycerol in potato starch matrix.

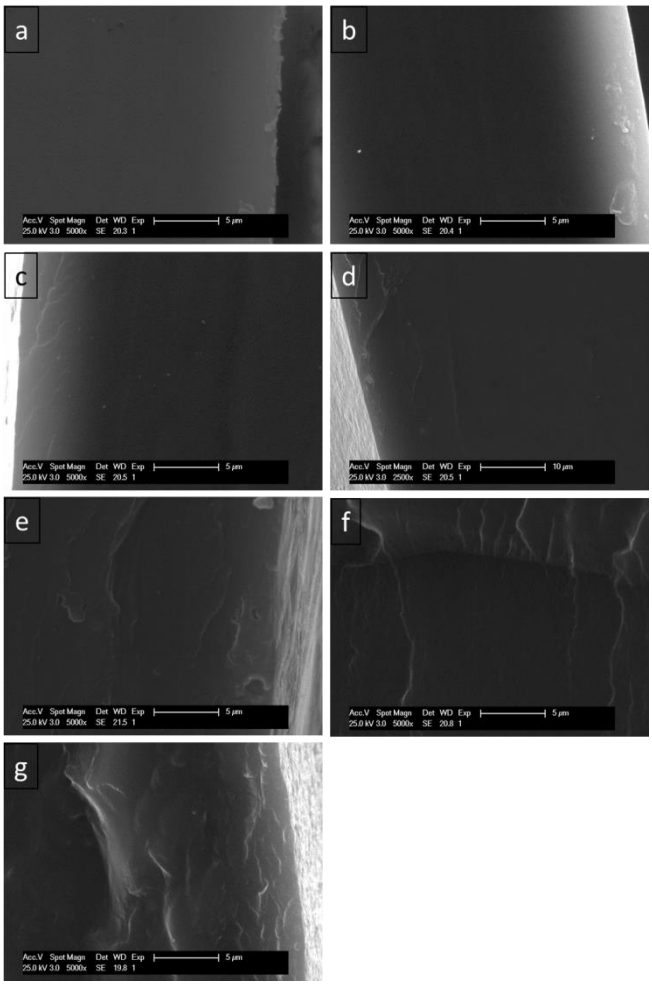

Fig. 7. SEM micrograph (5000x) of edible films cryo-fracture: (a) S-Gly0, (b) S-Gly15, (c) S-Gly25, (d) S-Gly35, (e) S-Gly35-Cat, (f) S-Gly35-SNC, (g) S-Gly35-Cat-SNC.

As expected, the cryo-fractured surface of catechin based biocomposite (Fig. 7.e) and the SNC bionanocomposites (Fig.7.f and g) appear to be more brittle and the absence of any evident SNC agglomeration was observed.

The thermal stability of the edible films was studied by thermogravimetric analysis conducted under isothermal mode during 60 min at 110 ºC which is the frequently extrusion temperature used for thermoplastic starches [40]. During the first 10 minutes of the experiment, which was the time required to reach 110 ºC, the edible films lost approximately 7 % of the initial mass due to the loss of the absorbed and bounded water. Initially, all additives improved the thermal stability of starch films, with the exception of S-Gly15 which lost around 8 % of the initial mass at 10 minutes probably due to the plasticizer evaporation. Higher amount of plasticizer (25 wt % and 35 wt %) slightly stabilized the starch matrix. At 10 minutes, S-Gly35-Cat was the most thermally stable edible film (5.5 % of mass loss) showing the effectiveness of the antioxidant to stabilize the starch matrix. However, after 30 minutes it showed a decrease on the thermal stability and, finally, it lost 8 % of the initial weight at 60 min. This findings suggest that the antioxidant capacity of catechin at the selected amount of 1 wt % protected the plasticized starch matrix from thermal degradation at the first stage, while after the consumption of catechin the degradation is accelerated [2]. Both nanocomposite films, S-Gly35-SNC and S-Gly35-Cat-SNC, showed an improvement on the thermal stability of neat S-Gly35 since their mass losses were lower than 0.5 % from 10 min, after the water evaporation, to 60 min, at the end of the whole isothermal TGA test.

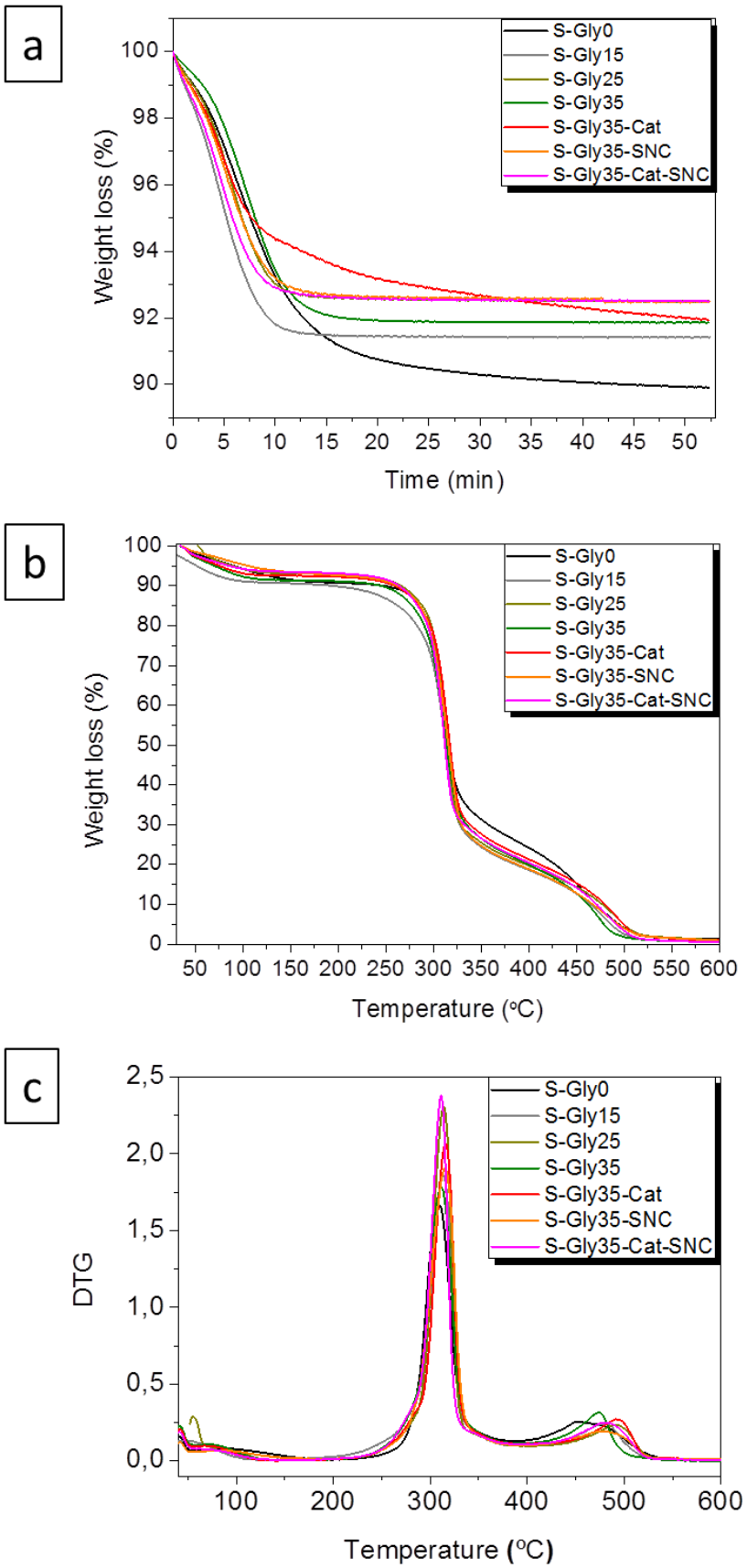

Fig. 8. Thermogravimetric analysis of edible films: (a) Isothermal TGA analysis. Dynamic: (b) TGA and (c) DTG.

The effect of Cat and SNC on the thermal properties of the plasticized starch films was also investigated by dynamic TGA measurements. The TGA and DTG curves are shown in Fig. 8.b and Fig. 8.c and the main thermal parameters obtained from these curves are summarized in Table 2. Starch based films showed three step degradation processes. The first step at temperatures around 100 ºC is related to the loss of bounded water in the film and low molecular weight compounds [12, 41]. The second weight loss, centered around 310º C, represents the main degradation process and is related to the cleavage of ether linkages in starch backbone [42] and, in the case of plasticized systems to the starch/glycerol reach phase [12]. Plasticized films showed lower onset degradation temperatures than unplasticized starch film (S-Gly0). The lower thermal stability caused by the presence of glycerol has been related with the reduction of the inter- and intra-molecular bonds interaction within the polymer matrix due to glycerol presence, resulting in a decrease of thermal stability of the whole system [16]. Cat and SNC produced an increase of the $T_{10\%}$ delaying the beginning of the thermal decomposition of starch/glycerol systems. The combined effect of Cat and SNC results in the bionanocomposite edible films with the highest thermal stability in which both particles delayed the beginning of the thermal decomposition process of about 20ºC. Glycerol slightly shifted the T_{maxI} values to lower temperatures. Both particles shifted the T_{maxI} and T_{maxII} of S-Gly35 films towards higher values. This effect was particularly evident in S-Gly35-Cat due to the antioxidant activity of Cat. Conversely to S-Gly35-Cat and S-Gly35-SNC, the effect of the addition of both particles, SNC and Cat, to the plasticized starch matrix resulted negligible in improving the thermal stability. This unexpected result can be related with the high amount of hydroxyl groups in the surfaces of both particles which are able to interact not only with the polymer matrix,

but also among them, reducing the possibility to further improve the thermal stability. Finally, the third weight loss step around 475º C has been related with the oxidation of the partially decomposed starch in air atmosphere [43]. At this stage, although plasticized starch films showed slightly higher T_{maxII} values, they were more susceptible to the degradation, thus contributing to a decrease of the mass loss in the third step with respect of the neat starch film (S-Gly0). The biocomposite and bionanocomposites edible films showed the same increase on the T_{maxII} than S-Gly35, showing some stabilization effect on the partially decomposed starch.

Table 2. TGA analysis of edible films

Edible films	**$T_{10\%}$ (ºC)**	**T_{maxI} (ºC)**	**T_{maxII} (ºC)**
S-Gly0	246.9	308.2	452.6
S-Gly15	193.0	313.4	481.9
S-Gly25	265.8	313.5	490.7
S-Gly35	244.8	311.6	474.1
S-Gly35-Cat	260.0	316.4	493.2
S-Gly35-SNC	262.3	314.3	480.2
S-Gly35-SNC-Cat	264.1	311.0	478.5

The mechanical properties of destructured starch are strongly influenced by the botanical origin of starch, more specifically the proportion of amylose and amylopectin [44]. The amylopectin based material presents a ductile behavior (high elongation at break), while those based on amylose shows a typical behavior of a brittle material, according with Lourdin et al. [44, 45]. In this work we used native potato starch as

matrix for the edible films with an amylose content between 26 and 28 % [46]. The stress-strain curves are shown in Fig. 9.

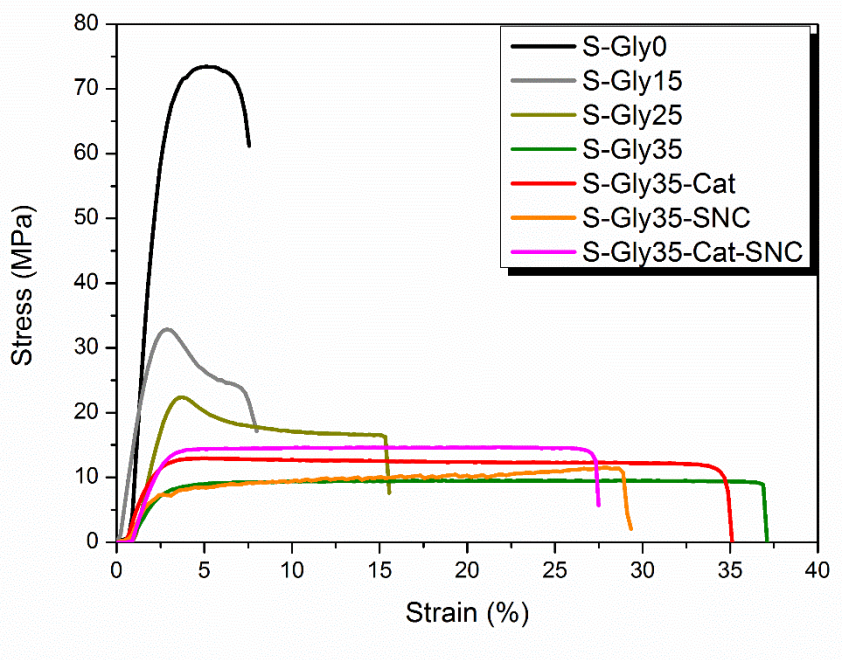

Fig. 9. Stress-strain curves of edible films

Because of this relative high amount of amylose and the high humidity dependence of starch, all the edible films displayed a rather brittle mechanical behavior even if a slight plastic deformation is observed when glycerol was added.

As expected, the tensile strength, strain at break and elastic modulus in starch edible films were affected by the glycerol content as it is shows in Fig.10. Tensile strength and elastic modulus decreased, while the elongation at break increased with increasing glycerol in all edible films, in agreement with Laohakunjit et al. [44]. Since these materials are intended for flexible films applications and the elongation at break increased with the amount of glycerol, particularly for 35 wt % formulation (Fig. 9- c), the bionanocomposites were developed by plasticizing starch matrix with 35 wt% of glycerol.

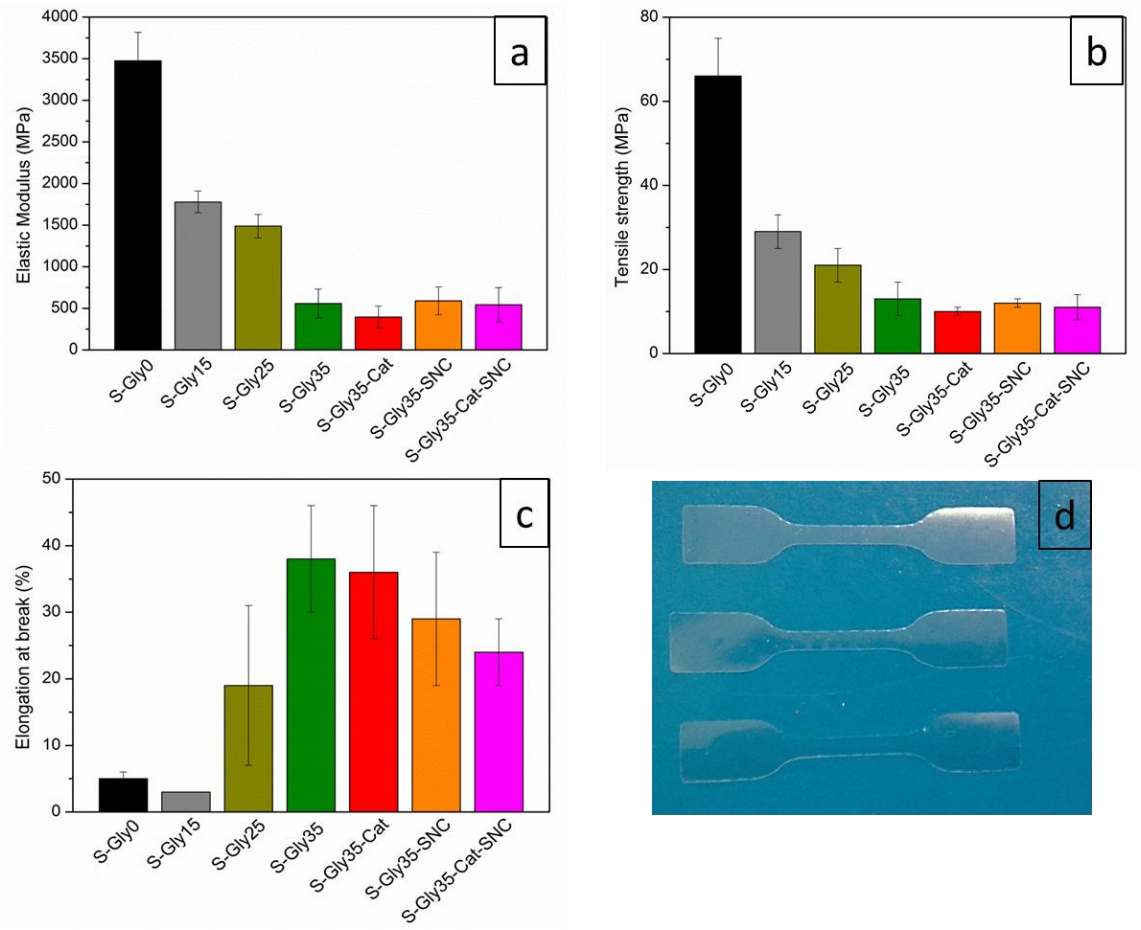

Fig. 10. Tensile properties of all the edible films: (a) Elastic Modulus, (b) Tensile strength and (c) Elongation at break. (d) Photograph of tensile test specimens.

In previous works it was demonstrated that catechin produces a reinforcing effect in case of both, traditional plastic composites such as polypropylene [47] and, also, biopolymers such as poly(lactic acid) (PLA) and poly(hydroxybutyrate) (PHB) [2]. In our case, when catechin was added, the biocomposite (S-Gly35-Cat) did not show significant changes respect of the mechanical performance of the neat counterpart (S-Gly35). This result can be explained by the low amount of catechin used to process the biocomposite that was not capable to improve the mechanical performance of the S-Gly35 film. However, when SNC have been added, a slightly increase in the elastic modulus maintaining quite constant the tensile strength has been obtained, in

comparison with the neat counterpart (S-Gly35). Moreover, when both catechin and SNC have been added, the S-Gly35-Cat-SNC show increased mechanical performance respect S-Gly35-Cat, thus confirming the reinforcing effect of SNC with the increase in brittleness of bionanocomposite cryo-fractured surfaces previously commented.

Disintegration in compost condition was studied. Fig. 11.a shows the visual appearance of edible films recovered at different composting times. As well, visual observations were confirmed by calculating the disintegration degree (weight loss) as a function of time (Fig. 11.b), where 90 % of disintegration was considered as the goal of samples disintegrability. All starch based films, showed a high degree of disintegration, being lower than 30 h for all films. It has been reported that the presence of amylopectin with branched hydroxylated chains favors hydration, water diffusion, and at last microorganism growth [48]. After 1h in compost the films became smaller. In general, after 1.5h of incubation, the edible films became breakable, particularly neat starch (S-Gly0) and plasticized starch with the lower amount of glycerol (S-Gly15). At 6h of disintegration it was observed that the edible film with lower amount of glycerol (S-Gly15) was the one that lost the higher amount of the initial weight, followed by the unplasticized film. This behaviour can be due to the fact that the plasticizer is able to increase the polymer chain mobility allowing the water infiltrating through the polymer matrix leading to earlier hydrolysis. Conversely, lower weight loss was observed for those samples with higher amount of glycerol (S-Gly25 and S-Gly35), probably due to the better interaction between starch and glycerol which results in a more homogeneous material. The addition of both, Cat and SNC delays the disintegration process of the biocomposite and bionanocomposite edible films, respectively. These results could be related with the fillers nucleation effect on the starch/glycerol matrix where increased

crystallinity decreased their degradation rate since the ordered structures in the crystalline fractions retain the action of microorganisms [49].

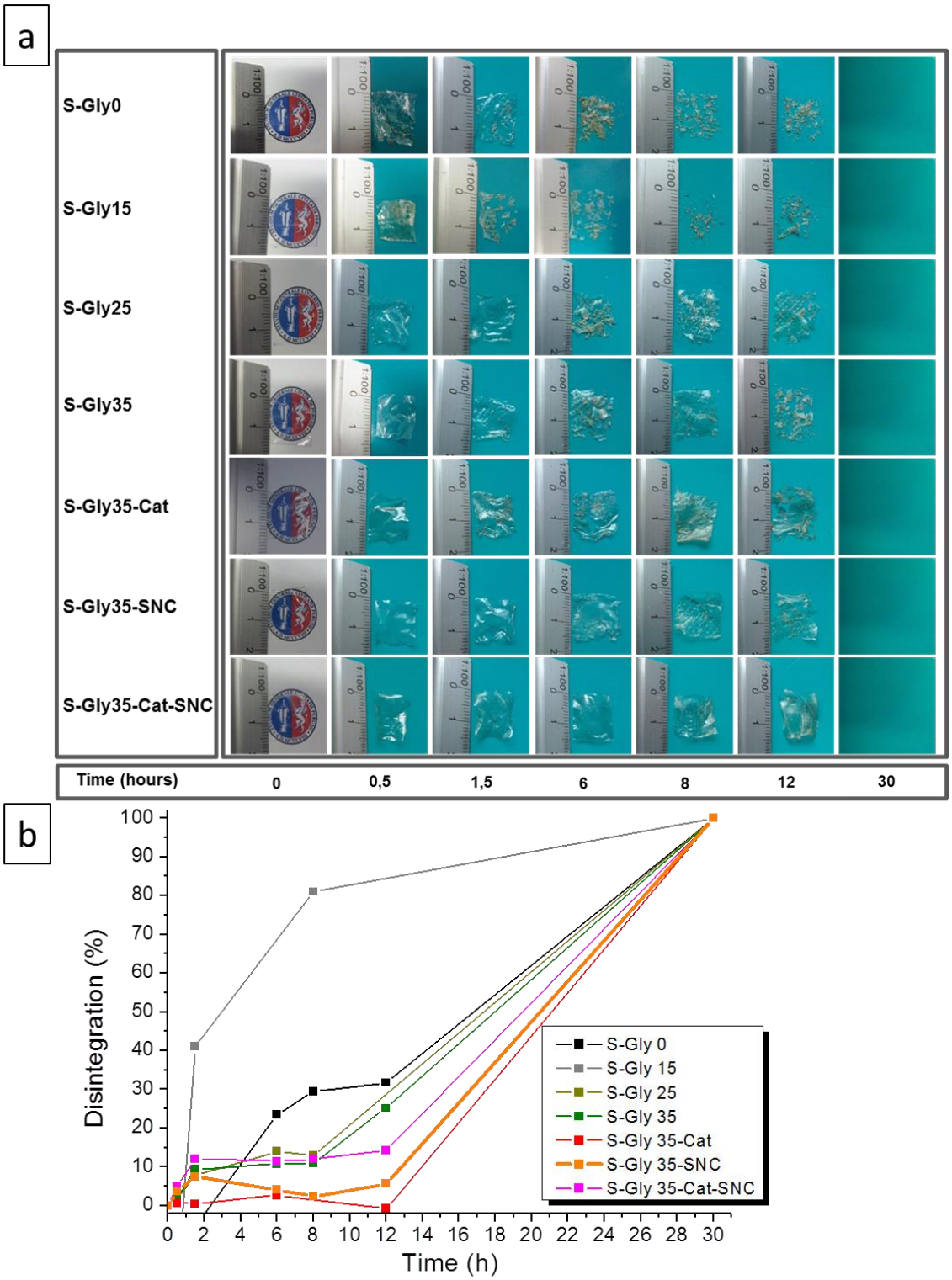

Fig. 11. (a) Visual appearance of edible films during disintegration. (b) Degree of disintegration of edible films under composting conditions as a function of time.

4. Conclusions

In this work the processing conditions and characterization of bionanocomposite edible films based on plasticized thermoplastic starch reinforced with the innovative combination of starch nanocrystals and the antioxidant catechin were studied. DSC analysis demonstrated that the optimal processing conditions to reach complete starch granules destructuration was 80 ºC for 15 minutes. The solvent casting process produced a complete destructuration of starch crystalline structure in the edible films, as revealed the X-ray diffraction pattern. Meanwhile, the isothermal TGA analysis showed that glycerol should be added at higher amount than 25 wt % for melt processing proposes. Moreover, as expected, the incorporation of glycerol as plasticizer favors the stretchability of the edible films. SNC were synthesized from waxy maize starch by means of sulfuric acid hydrolysis. The TGA of SNC suspensions adjusted to pH 7, pH 9 and pH 11 showed a higher thermal stability for the neutral SNC (pH 7), in which the sulfate ester groups on the surface of the SNC where more stable. Consequently, transparent homogeneous plasticized edible films were obtained by adding 1 wt % of SNC at pH 7 as well as 1 wt % of catechin. Moreover, the synergetic effect of both micro and nanofillers was studied by incorporating both catechin and SNC in the same bionanocomposite edible film. The influence of catechin and starch nanocrystals addition on their structural, thermal and mechanical properties was studied. Biocomposite S-Gly35-Cat and bionanocomposites, S-Gly35-SNC and S-Gly35-Cat-SNC, showed a more roughness fracture surface due to the reinforcing effect of the additives. The addition of Cat considerably improved the thermal stability of the edible films, while SNC presence improved their mechanical performance. The bionanocomposite S-Gly35-Cat-SNC showed the best properties for the intended use as edible films for possible food packaging, with considerably higher thermal stability and

a slightly improvement on the mechanical performance. The disintegrability test under composting conditions confirmed the biodegradable character of all edible film formulations.

Regarding to all these results, it can be concluded that the combination of plasticized starch matrix loaded with both, SNC and Cat particles, leads to a bionanocomposite material that may offer good perspective for industrial processing as biobased transparent flexible film, with enhanced thermal and mechanical properties, biodegradable in compost and, thus, suitable for biodegradable edible films for food packaging applications.

Acknowledgments

We are indebted to the Spanish Ministry of Economy and Competitiveness (MAT2013-48059-C2-1-R and MAT2014-55778-REDT) and to the Regional Government of Madrid (S2013/MIT-2862) for their economic support. L.P. and M.P.A. acknowledge MINECO for the "Ramon y Cajal" and "Juan de la Cierva" contracts, respectively.

References.

[1] Avérous L. Biodegradable multiphase systems based on plasticized starch: a review. J Macromol Sci Part C, Polym Rev 2004;44:231-74.

[2] Arrieta MP, Castro-López MadM, Rayón E, Barral-Losada LF, López-Vilariño JM, López J, et al. Plasticized poly (lactic acid)–poly (hydroxybutyrate)(PLA–PHB) blends incorporated with catechin intended for active food-packaging applications. J Agric Food Chem. 2014;62:10170-80.

[3] Jiménez A, Fabra MJ, Talens P, Chiralt A. Effect of sodium caseinate on properties and ageing behaviour of corn starch based films. Food Hydrocolloid. 2012;29:265-71.

[4] Sanchez-Garcia MD, Lagaron JM. On the use of plant cellulose nanowhiskers to enhance the barrier properties of polylactic acid. Cellulose. 2010;17:987-1004.

[5] Lu D, Xiao C, Xu S. Starch-based completely biodegradable polymer materials. Express Polym Lett. 2009;3:366-75.

[6] LeCorre D, Bras J, Dufresne A. Influence of botanic origin and amylose content on the morphology of starch nanocrystals. J Nanopart Res. 2011;13:7193-208.

[7] Wang TL, Bogracheva TY, Hedley CL. Starch: as simple as A, B, C? J Exp Bot. 1998;49:481-502.

[8] Janssen L, Moscicki L. Thermoplastic starch as packaging material. Acta Scientiarum Polonorum Technica Agraria. 2006;5:19.

[9] Chen B, Evans JR. Thermoplastic starch–clay nanocomposites and their characteristics. Carbohydr Polym 2005;61:455-63.

[10] Le Corre D, Bras J, Dufresne A. Starch nanoparticles: A review. Biomacromolecules. 2010;11:1139-53.

[11] LeCorre D, Bras J, Dufresne A. Influence of native starch's properties on starch nanocrystals thermal properties. Carbohydr Polym. 2012;87:658-66.

[12] García NL, Ribba L, Dufresne A, Aranguren M, Goyanes S. Effect of glycerol on the morphology of nanocomposites made from thermoplastic starch and starch nanocrystals. Carbohydr Polym. 2011;84:203-10.

[13] Angellier H, Molina-Boisseau S, Dole P, Dufresne A. Thermoplastic starch-waxy maize starch nanocrystals nanocomposites. Biomacromolecules. 2006;7:531-9.

[14] Galicia-García T, Martínez-Bustos F, Jiménez-Arevalo O, Martínez A, Ibarra-Gómez R, Gaytán-Martínez M, et al. Thermal and microstructural characterization of biodegradable films prepared by extrusion–calendering process. Carbohydr Polym. 2011;83:354-61.

[15] Jiménez A, Fabra MJ, Talens P, Chiralt A. Edible and biodegradable starch films: a review. Food Bioprocess Tech. 2012;5:2058-76.

[16] Arrieta MP, Peltzer MA, del Carmen Garrigós M, Jiménez A. Structure and mechanical properties of sodium and calcium caseinate edible active films with carvacrol. J Food Eng. 2013;114:486-94.

[17] Fernández-Pan I, Maté J, Gardrat C, Coma V. Effect of chitosan molecular weight on the antimicrobial activity and release rate of carvacrol-enriched films. Food Hydrocolloid. 2015;51:60-8.

[18] Arrieta MP, Peltzer MA, López J, del Carmen Garrigós M, Valente AJ, Jiménez A. Functional properties of sodium and calcium caseinate antimicrobial active films containing carvacrol. J Food Eng. 2014;121:94-101.

[19] Peponi L, Puglia D, Torre L, Valentini L, Kenny JM. Processing of nanostructured polymers and advanced polymeric based nanocomposites. Mater Sci Eng, R. 2014;85:1-46.

[20] Castro-López MdM, López-Vilariño JM, González-Rodríguez MV. Analytical determination of flavonoids aimed to analysis of natural samples and active packaging applications. Food Chem. 2014;150:119-27.

[21] Lopez de Dicastillo C, Castro-López MdM, Lasagabaster A, López-Vilariño JM, González-Rodríguez MV. Interaction and release of catechin from anhydride maleic-grafted polypropylene films. ACS Appl Mater Interfaces. 2013;5:3281-9.

[22] Raquez J-M, Habibi Y, Murariu M, Dubois P. Polylactide (PLA)-based nanocomposites. Prog Polym Sci. 2013;38:1504-42.

[23] Peponi L, Valentini L, Torre L, Mondragon I, Kenny JM. Surfactant assisted selective confinement of carbon nanotubes functionalized with octadecylamine in a poly(styrene-b-isoprene-b-styrene) block copolymer matrix. Carbon. 2009;47:2474-80.

[24] Chang PR, Jian R, Yu J, Ma X. Starch-based composites reinforced with novel chitin nanoparticles. Carbohydr Polym. 2010;80:420-5.

[25] Angellier H, Choisnard L, Molina-Boisseau S, Ozil P, Dufresne A. Optimization of the preparation of aqueous suspensions of waxy maize starch nanocrystals using a response surface methodology. Biomacromolecules. 2004;5:1545-51.

[26] UNE. UNE-EN ISO-20200. Determination of the degree of disintegration of plastic materials under simulated composting conditions in a laboratory-scale test. 2006.

[27] Bogracheva TY, Morris V, Ring S, Hedley C. The granular structure of C-type pea starch and its role in gelatinization. Biopolymers. 1998;45:323-32.

[28] Imberty A, Chanzy H, Perez S, Buleon A, Tran V. New three-dimensional structure for A-type starch. Macromolecules. 1987;20:2634-6.

[29] Imberty A, Perez S. A revisit to the three-dimensional structure of B-type starch. Biopolymers. 1988;27:1205-21.

[30] Aggarwal P, Dollimore D. The combustion of starch, cellulose and cationically modified products of these compounds investigated using thermal analysis. Thermochim Acta 1997;291:65-72.

[31] Wei B, Xu X, Jin Z, Tian Y. Surface chemical compositions and dispersity of starch nanocrystals formed by sulfuric and hydrochloric acid hydrolysis. PloS one. 2014;9:e86024.

[32] Russell PL. Gelatinisation of starches of different amylose/amylopectin content. A study by differential scanning calorimetry. J Cereal Sci 1987;6:133-45.

[33] Tako M, Hizukuri S. Gelatinization mechanism of potato starch. Carbohydr Polym 2002;48:397-401.

[34] Shiotsubo T. Gelatinization temperature of potato starch at the equilibrium state. Agric Biol Chem. 1984;48:1-7.

[35] Ratnayake WS, Jackson DS. A new insight into the gelatinization process of native starches. Carbohydr Polym 2007;67:511-29.

[36] Lopez-Rubio A, Flanagan BM, Gilbert EP, Gidley MJ. A novel approach for calculating starch crystallinity and its correlation with double helix content: A combined XRD and NMR study. Biopolymers. 2008;89:761-8.

[37] Lafargue D, Pontoire B, Buléon A, Doublier JL, Lourdin D. Structure and mechanical properties of hydroxypropylated starch films. Biomacromolecules. 2007;8:3950-8.

[38] Morán JI, Cyras VP, Giudicessi SL, Erra-Balsells R, Vázquez A. Influence of the glycerol content and temperature on the rheology of native and acetylated starches during and after gelatinization. J Appl Polym Sci 2011;120:3410-20.

[39] Park HM, Li X, Jin CZ, Park CY, Cho WJ, Ha CS. Preparation and properties of biodegradable thermoplastic starch/clay hybrids. Macromol Mater Eng 2002;287:553-8.

[40] Park H-M, Lee W-K, Park C-Y, Cho W-J, Ha C-S. Environmentally friendly polymer hybrids Part I Mechanical, thermal, and barrier properties of thermoplastic starch/clay nanocomposites. J Mater Sci 2003;38:909-15.

[41] Moreno O, Atarés L, Chiralt A. Effect of the incorporation of antimicrobial/antioxidant proteins on the properties of potato starch films. Carbohydr Polym. 2015;133:353-64.

[42] Palanikumar S, Siva P, Meenarathi B, Kannammal L, Anbarasan R. Effect of Fe 3 O 4 on the sedimentation and structure–property relationship of starch under different pHs. Int J Biol Macromol 2014;67:91-8.

[43] Wilhelm H-M, Sierakowski M-R, Souza G, Wypych F. Starch films reinforced with mineral clay. Carbohydr Polym 2003;52:101-10.

[44] Hulleman SHD, Janssen FHP, Feil H. The role of water during plasticization of native starches. Polymer. 1998;39:2043-8.

[45] Lourdin D, Valle GD, Colonna P. Influence of amylose content on starch films and foams. Carbohydr Polym 1995;27:261-70.

[46] Stawski D. New determination method of amylose content in potato starch. Food Chem 2008;110:777-81.

[47] López de Dicastillo C, Castro-López MdM, Lasagabaster A, López-Vilariño JM, González-Rodríguez MV. Interaction and Release of Catechin from Anhydride Maleic-Grafted Polypropylene Films. ACS Appl Mater Interfaces. 2013;5:3281-9.

[48] Rodrigues CA, Tofanello A, Nantes IL, Rosa DS. Biological Oxidative Mechanisms for Degradation of Poly (lactic acid) Blended with Thermoplastic Starch. ACS Sustain Chem Eng. 2015.

[49] Arrieta M, Fortunati E, Dominici F, Rayón E, López J, Kenny JM. PLA-PHB/cellulose based films: mechanical, barrier and disintegration properties. Polym Degrad Stabil. 2014;107:139-49.